Dynamic mode optimization for the deposition of homogeneous TiO2 thin film by atmospheric pressure PECVD using a microwave plasma torch

Amelie Perraudeau, Christelle Dublanche-Tixier, Pascal Tristant, Christophe Chazelas

Dynamic mode optimization for the deposition of homogeneous TiO_2 thin film by atmospheric pressure PECVD using a microwave plasma torch.

Amélie Perraudeau*, Christelle Dublanche-Tixier, Pascal Tristant, Christophe Chazelas.
Université de Limoges, CNRS, IRCER, UMR 7315, Centre Européen de la Céramique, 16 rue Atlantis, F-87000 Limoges, France
*Corresponding author
Amélie Perraudeau : amelie.perraudeau@unilim.fr
Christelle Dublanche-Tixier : christelle.tixier@unilim.fr
Pascal Tristant : pascal.tristant@unilim.fr
Christophe Chazelas : christophe.chazelas@unilim.fr

Abstract

An atmospheric pressure plasma-enhanced chemical vapor deposition process using a microwave plasma torch has been used for titania thin film synthesis. A dynamic deposition mode was set up to cover a square centimeter surface with a nanostructured TiO_2 film. The process parameters were studied and optimized to control the coating crystallinity and morphology and limit the formation of powder in the plasma phase. Contrary to static deposition, the substrate movement promotes a film growth by particles agglomeration in the reference conditions, leading to a cauliflower-like morphology. Then, the precursor proportion in the plasma appears to be determinant in the TiO_2 film microstructure. For a precursor flow rate beyond 0.2 slpm, the titania nanoparticles formation in the gas phase is promoted and the thin film is growing by particles agglomeration, leading to a columnar cauliflower-like morphology. At a flow rate of 0.2 slpm, the growth by surface reaction is promoted and the TiO_2 film is columnar, where each column is an anatase crystal. After the optimization of the substrate holder movement, it was possible to deposit this last microstructure homogeneously on a square centimeter surface.

1. Introduction

Titanium dioxide TiO_2 is nowadays a material of great interest. It might crystallize under different phases: (i) rutile which is thermodynamically stable, (ii) anatase and (iii) brookite both considered as metastable. The crystalline phase determines the final properties of the synthesized thin films. The high band gap of TiO_2 makes it suitable for numerous applications using its photocatalytic activity for self-cleaning surfaces [1,2], water or air purification [3] and/or hydrogen production [4]. Titania is also used in photovoltaics to convert solar energy into electricity in dye-sensitized solar cells [5,6] or perovskite solar cells [7,8]. The transparency and the high refractive index of TiO_2 can be profitable for anti-reflective coatings [9,10] or interference filters [11].

The most studied routes to synthesize TiO_2 thin films are sol-gel processes [12,13], reactive sputtering [14,15] and chemical vapor deposition (CVD) [16,17]. The latest is based on the decomposition of gaseous precursors to generate a chemical reaction heating the substrate. A plasma activation may also be used (plasma enhanced CVD – PECVD) to decrease the substrate temperature. Most of the time these processes are carried out at low pressure, usually around 0.01 to 1 kPa, where the reactions are well-controlled, and the coating characteristics are well-known. Atmospheric pressure CVD processes (AP-PECVD) were investigated in the past few years to avoid expensive vacuum systems and increase process flexibility [18]. At atmospheric pressure, more collisions are generated between reactive species in the plasma phase. Before reaching the substrate, they can react and create clusters by homogeneous reactions. These powders are transported to the substrate and can interfere with the film growth and be embedded in the layer.

This phenomenon is amplified when pressure and/or plasma power are increased [19]. Atmospheric pressure also causes plasmas contraction, as flames for PECVD plasma torches. Two different zones are noticeable in these plasmas: (i) the central zone called the core, the most reactive area of the flame, and (ii) the peripheral zone called the plume. This plasma shape is defined by temperature and composition gradients from the plasma center to the plasma plume and thus leads to the deposition of localized coatings [20]. Thus, the substrate movement is necessary to achieve a larger uniform coating surface to investigate film properties.

Few teams like Maurau *et al.* [21] and Boscher *et al.* [22] used a blown arc discharge to deposit titania moving the substrate in front of the plasma jet. The obtained columnar films had a cauliflower structure and were amorphous. Agglomerates formed in the plasma were also present and appeared to be partially crystallized under the anatase phase. Fakhouri *et al.* [23] elaborated ballistic columnar amorphous titania films with an open-air atmospheric pressure plasma jet (APPJ) moving on top of the substrate. A mixture of anatase and rutile was obtained after annealing, enhancing the films properties.

This study deals with the deposition of a homogeneous titania film on a square centimeter surface. In a previous study [20] working parameters were defined for deposition with a microwave plasma torch in the static mode, where the substrate was stationary facing the plasma. In this work, the influence of the substrate holder movement (*i.e.,* dynamic mode) on the microstructure and the crystallization of the TiO_2 films were investigated, trying to limit cluster formation in the plasma phase. The process parameters were optimized and titania films were characterized. Dynamic and static growth mechanisms were compared to understand the formation of a few square centimeter surface coating, suitable for applications like photovoltaic cells.

2. Experimental details

2.1. Experimental setup

The AP-PECVD system used in this study is an axial injection torch (TIA), represented on Fig. 1. Microwaves are provided by a SAIREM 1200 KED generator (2,45 GHz) and transported by a rectangular waveguide to supply the cylindrical outer conductor of the coaxial guide. The nozzle, with a 2 mm inner diameter, is placed on the top of the coaxial conductor in a large cylindrical open-air reactor. An exhaust device removes gas or particles produced during the deposition. The substrate holder faces the plasma jet and can be moved along the x and y-axis using a Labview® program. Its height can be changed manually.

Argon (AirLiquide Alphagaz I, purity >99.999%) was used as plasma gas. Oxygen required to form titania films was provided by the ambient air, which was well incorporated into the discharge according to the previous optical emission spectroscopy studies [24,25]. The titanium tetraisopropoxide (TTIP), organometallic precursor (Alfa Aesar, $Ti(OC_3H_7)_4$, purity >97%) was kept into a 300-mL container under argon atmosphere, heated at a constant temperature of 37°C. Argon gas bubbled into the container and went out saturated with TTIP into the stainless steel gas lines, maintained at a temperature of 70°C to avoid the precursor vapor condensation during the transport. The TTIP flow rate was fixed by the argon flowrate bubbling into the container. The plasma gas and the carrier gas were mixed in the lines and transported through the inner conductor of the coaxial line to reach the nozzle. Parts of (100) monocrystalline silicon wafers were used as substrates. They were cleaned before coating with an optical paper and ethanol. In this study, all the coatings were elaborated in dynamic mode, meaning that the substrate holder is moving during the deposition.

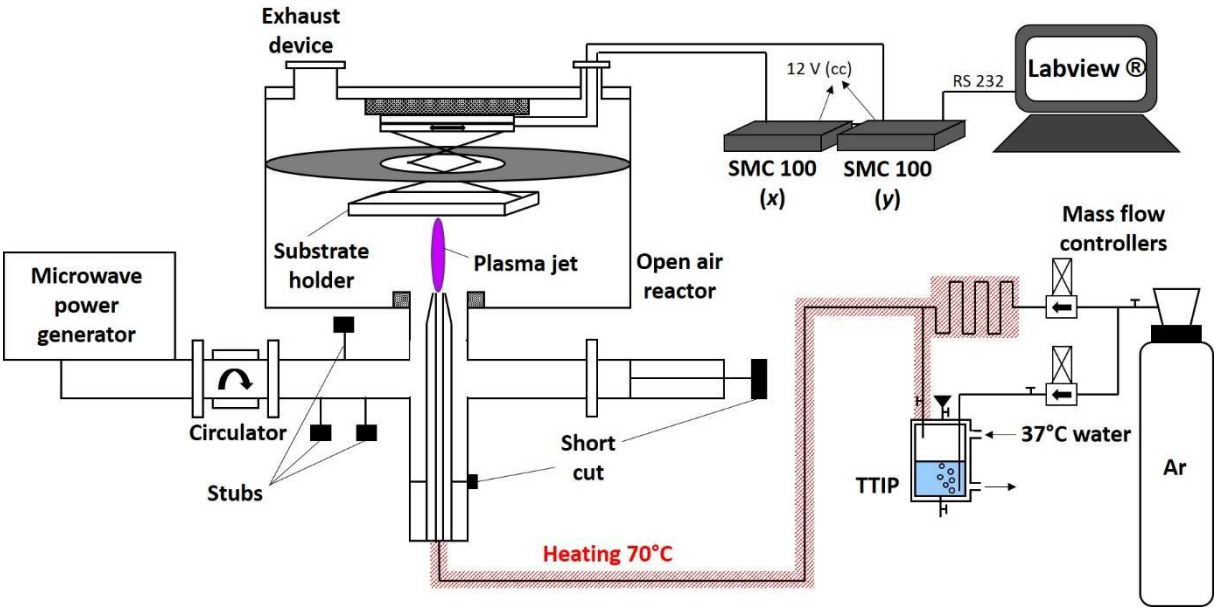

Fig. 1. Schematic representation of the AP-PECVD microwave plasma torch.

2.2. Analytical methods

First, the morphologies of the titania films were observed using a field emission scanning electron microscope (FESEM) Quanta 450 FEG FEI with an operating range of 15 kV. A 5-nm platinum coating covered the analyzed surfaces before observations. X-Ray diffraction (XRD) was used to determine the crystallinity of the films. The apparatus is a D8 Advance from Bruker, with a θ-2θ configuration using the Cu K_α filtered radiation (0.154 nm). The measurements were performed between 20° and 60°, and the sample was spinning at 15 rpm. A high-resolution transmission electron microscope (HRTEM) JEOL 2100F with an operating voltage of 200 kV was used to complete the analysis. The samples were prepared by removing the coating from the silicon substrates with a stainless-steel tip. The fragments were mixed in water and deposited on a copper grid for observation.

2.3. Optimization methodology for titania film deposition

In the previous studies [20,24,26], the influence of the process parameters was investigated in static mode to control the thin film growth and to obtain a TiO_2 columnar thin film composed of aligned monocrystals. It was shown that the microwave power permits to control the film densification and limit the homogeneous nucleation in the gas phase. These requirements can be achieved with a power between 250 and 500 W, but a compromise is necessary to have sufficient energy to obtain a crystallized coating. In dynamic mode, the power was set to 420 W to ensure plasma stability during the substrate movement. The distance between the nozzle and the substrate should be adjusted between 10 and 30 mm to optimize the residence time of the species into the plasma to avoid the formation of powder in the gas phase. When this distance increases, the microstructure is affected due to particles embedded into the coating and the coating becomes amorphous. It was fixed to 10 mm which gave the best results for the previous studies. The gas flow rates had a strong influence on the coating growth and the particles formation in the plasma. The plasma gas flow rate was fixed at 17 slpm to ensure the precursor dilution and promote the film growth instead of the formation of non-adherent powder. The TTIP flow rate was initially fixed to 0.7 slpm.

For this study, the deposition of a few square centimeter surface titania coating with a controlled microstructure was the main challenge. The substrate holder displacement was first carried out on the *x*-axis to obtain a coating line as presented in Fig. 2. Three moving velocities were tested: 1, 3 and

5 mm/s in accordance with other studies [21–23,27]. As the moving velocity increases from 1 to 5 mm/s, more passes are necessary to achieve the same film thickness. The films presented interference fringes related to radial thickness inhomogeneities, already noticeable in static mode. The homogeneous thicker part at the center of the film represented a 1 mm large line and was the observed zone for SEM analysis.

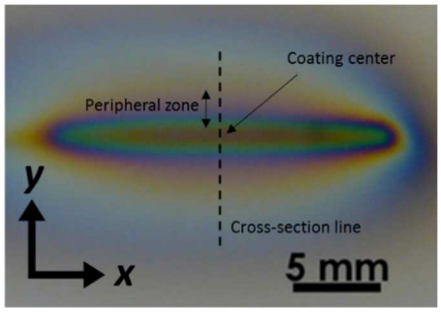

Fig. 2. Photograph of a coating line elaborated at 0.7 slpm of TTIP, a speed of 1 mm/s, doing 16 passes.

3. Results and discussion

3.1. Substrate movement influence on the film growth

The Fig. 3 shows the SEM images of 300 nm thick coatings elaborated at different velocities. The titania films are columnar, but contrary to the static mode where coatings were composed of aligned monocrystals [20], the columns are composed of nanoparticles, with a diameter of 10 to 20 nm, and exhibit a cauliflower-like structure. When the velocity was decreased to 1 mm/s, the columns seemed more regular and organized.

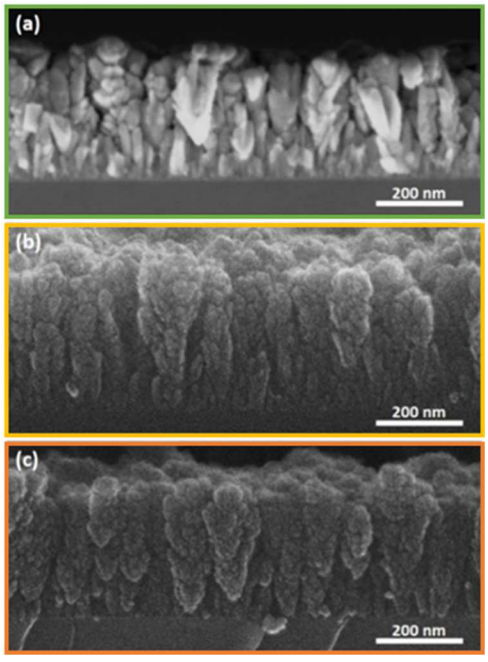

Fig. 3. Cross-sectional FESEM morphologies of titania films elaborated at a moving speed of (a) 5 mm/s doing 64 passes, (b) 3 mm/s doing 32 passes and (c) 1 mm/s doing 16 passes.

As mentioned in [20], two phenomena are competing in static mode during the film growth : (i) the surface reaction in the center of the coating, characterized by facetted columns, and (ii) the nanoparticles agglomeration in the peripheral zones as cauliflower-like columns. Regarding the microstructures on Fig. 3, the substrate movement appears to promote the growth by particles

agglomeration all over the coating. Titania nanoparticles would be formed in the plasma fringes and deposited on the substrate *via* gas recirculation implied both by the gas flow and the substrate displacement. Since reactive species were also reaching the substrate, the nanoparticles were glued and organized in cauliflower-like columns (Fig. 4).

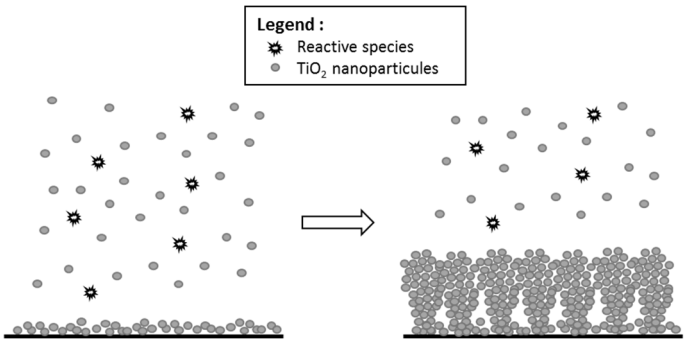

Fig. 4. Growth model for the cauliflower microstructure.

According to the XRD patterns on Fig. 5, each coating is polycrystalline with the signatures of the anatase phase (JCPDS 21-1272) and the rutile phase (JCPDS 21-1276). They all present a majority of anatase signature and a preferred orientation along the A(101) plan. In most studies [2,21–23,27–31], the as-deposited titania films are amorphous or partially crystallized and annealing is necessary to enhance the coating crystallinity. The TIA thus appears as a performing process to get ready-to-use coatings without any post-treatment.

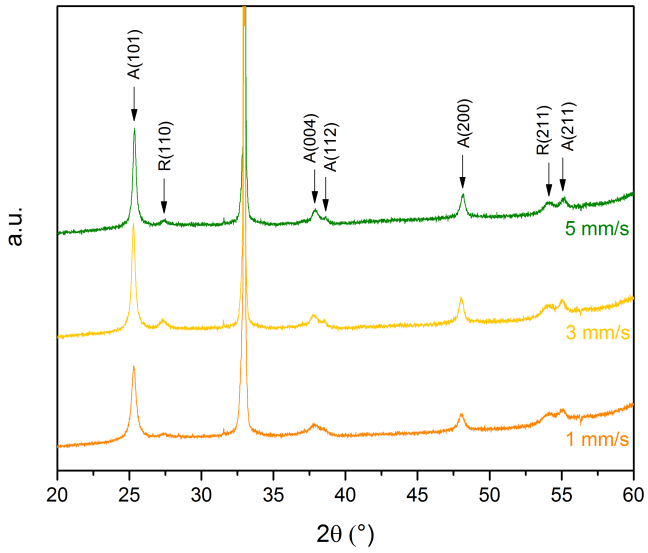

Fig. 5. Growth model for the cauliflower microstructure.

3.2. Titanium precursor flow rate influence on the film growth mechanisms

The control of the precursor quantity in the plasma phase should help to limit the homogeneous nucleation and promote a film growth by surface reaction. To this end, TTIP flow rates of 0.5, 0.3 and 0.2 slpm were tested and compared to the reference point elaborated at 0.7 slpm. The films were elaborated with 16 passes at 1 mm/s in front of the plasma along the *x*-axis. On Fig. 6 a-c-e-g, the film surfaces seem to evolve from cauliflower-like structures to facetted grains when the precursor flow rate is decreased and thus evolve from a particles agglomeration growth mechanism to surface reaction. The cross-section images of the films (Fig. 6 b-d-f-h) display a columnar structure in each case. For the flow rates of 0.7, 0.5 and 0.3 slpm, the columns are composed of nanoparticles with a

diameter from 10 to 20 nm. The coating elaborated at 0.2 slpm presents titania grains 50 nm high, 45 nm wide and 25 nm thick. The lower is the TTIP flow rate, and the thinner becomes the film. A thicker film at a flow rate of 0.2 slpm of TTIP precursor was realized with the same parameters and doing 60 passes to confirm the growth mechanism. As shown in Fig. 7, the film exhibits a rice-like surface and is composed of smooth facetted columns 350 nm high, 90 nm wide and 50 nm thick, with an intercolumnar porosity around 10 nm. A smaller columns population (50 to 100 nm high) is observed on the film base. This bimodal structure was already described in low-pressure TiO_2 synthesis by PECVD [28]. In their study, Ana Borras *et al.* established a growth model for polycrystalline titania inspired by the Kolmogorov model, represented in Fig. 8. After the nucleation step, each nucleus develops at the same growth rate. The most stable crystalline plans are then grown in bigger columns, giving a preferred orientation to the film. The other columns development is stopped, and thus two columns populations are visible.

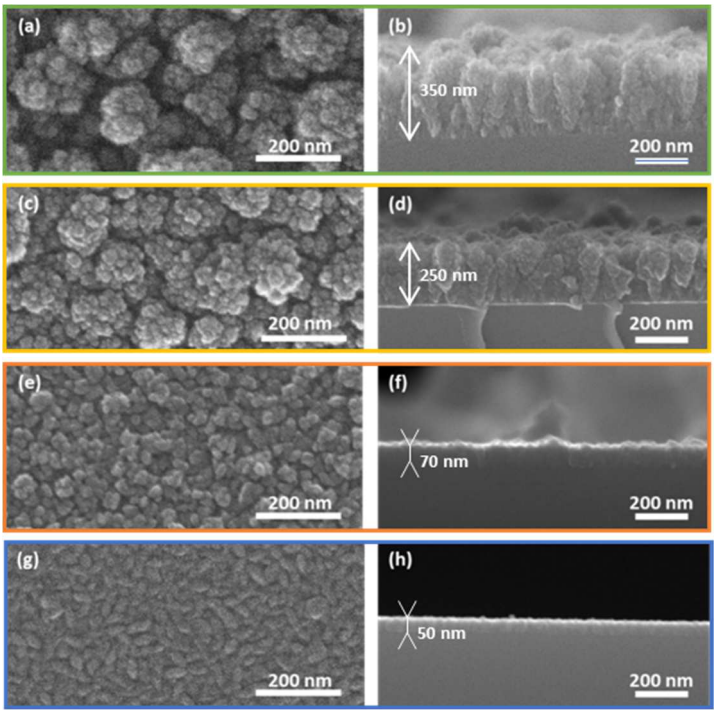

Fig. 6. Surface and cross-sectional FESEM images of titania coatings elaborated at different TTIP flow rates: (a)-(b) 0.7 slpm, (c)-(d) 0.5 slpm, (e)-(f) 0.3 slpm and (g)-(h) 0.2 slpm.

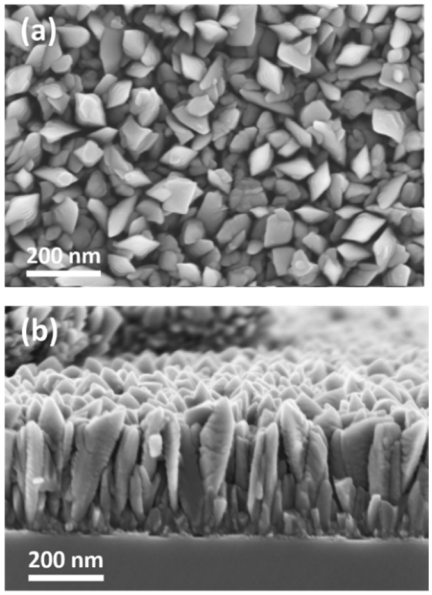

Fig. 7. FESEM images of the 60 passes optimized titania film, (a) top view and (b) cross-section.

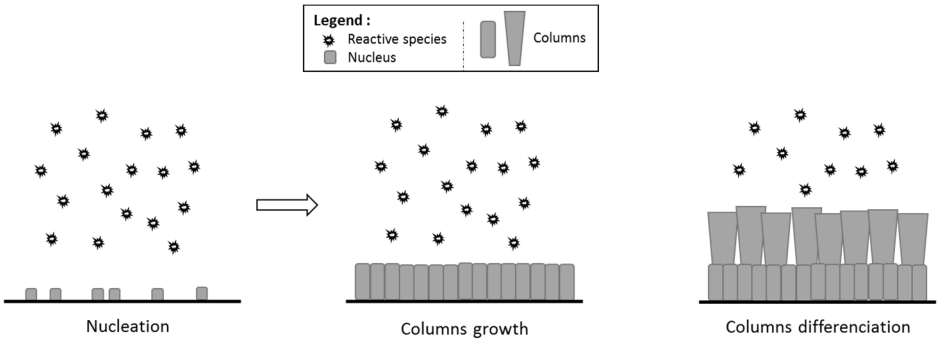

Fig. 8. Growth model for the facetted microstructure inspired by [28]

The XRD patterns on Fig. 9 and Fig. 10 display the polycrystalline nature of all the films. They are mostly crystallized under the anatase phase with a more important rutile signature appearing for the films elaborated at low TTIP flow rates. In each case, a preferred orientation along the (101) anatase plan is observed. Considering the dominant peaks of anatase and rutile phases, (101) and (110) respectively, it is possible to calculate the proportions of each phase in the film [23,32] with the equation (1):

$$f_A = \frac{1}{1 + \frac{1}{K}\frac{I_R}{I_A}} \quad (1)$$

where f_A is the fraction of anatase, K is a constant ($K = 0.79$ for $f_A > 0.2$ and $K = 0.68$ for $f_A < 0.2$), I_R is the intensity of the (110) rutile peak and I_A the intensity of the (101) anatase peak.

The fraction of rutile f_R can be then calculated following the equation (2):

$$f_R = 1 - f_A \quad (2)$$

The coatings deposited at 0.7 and 0.5 slpm of TTIP were composed of 90 % of anatase phase and 10 % of rutile phase. The film deposited at 0.3 slpm of TTIP was composed of 70 % of anatase and 30 % of rutile. The two films deposited at 0.2 slpm were composed of 50 % of anatase phase and 50 % of

rutile phase. When the TTIP flow rate decreases, fewer molecules have to be decomposed. More energy from the plasma would be available as a thermal component locally transferred to the growing film. This phenomenon could then contribute to the phase transition of the grains from anatase to rutile. However, these hypotheses should be taken carefully considering that the interactions between a substrate surface and the TIA plasma are not well-known yet in deposition mode.

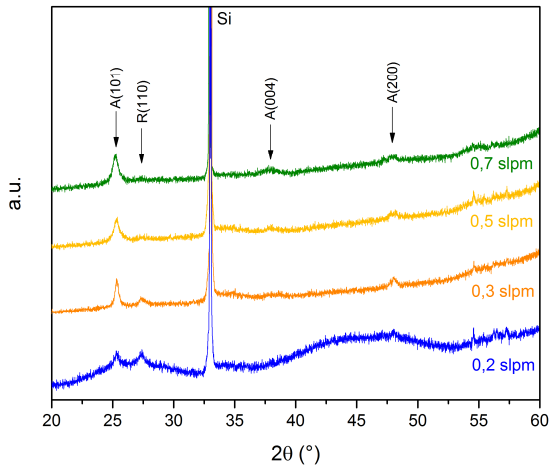

Fig. 9. XRD patterns of titania films elaborated at different TTIP flow rates.

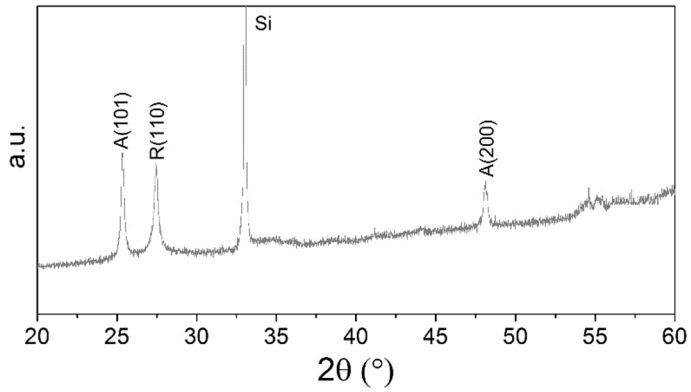

Fig. 10. XRD pattern of the 60 passes titania film elaborated in the optimized conditions.

TEM observations were performed on the thick coating deposited at a TTIP flow rate of 0.2 slpm to investigate the crystallinity of the columns. In static mode [20], the rice-like structure was typical of facetted columns, and each column was a TiO_2 monocrystal. The Fig. 11 shows an HRTEM micrography focused on one column of the coating, and as predicted each one of them is a titania monocrystal. This kind of organized microstructure is original regarding the amorphous columns composed of nanoparticles obtained in other studies [21–23].

Beside radial thickness variations, the TIA discharge is known to produce coatings exhibiting microstructure evolution from surface reaction growth in the center to nanoparticles agglomeration arrangements in the peripheral zone [20]. The optimized film (1 mm/s, 60 passes, 0.2 slpm of TTIP) was observed by SEM on a cross-section, as schemed on Fig. 2. Fig. 12 displays the evolution of the film microstructure from its center (*r = 0*) to its peripheral zone. The facetted columns appeared to be very similar on the first 1200 µm radius. The film thickness is gradually decreased from 350 nm to 200 nm in this zone. At *r = 1800 µm*, it seems that there is only a small facetted columns population, meaning probably that the peripheral film zone was not at the same growing stage than the film

center. This growth difference could be explained by the reactive species gradient existing radially in the discharge [25]. Fewer titanium atoms are available in the peripheral zone of the discharge to contribute to the film growth, and thus the growth rate is reduced. The parameters optimization in dynamic mode permitted to get rid of the influence of the plasma gradients on the coating microstructure in given conditions. Thus, it seems possible to deposit a second line at around 1 mm away from the center of the first one to continue the columns growth and obtain monocrystals on a larger surface to have a 1 cm² coating.

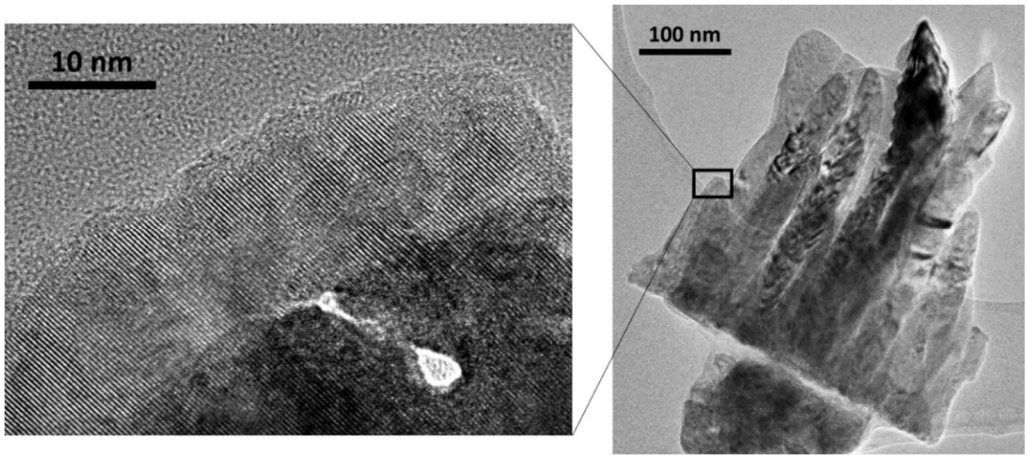

Fig. 11. HRTEM images of the optimized titania film elaborated at 1 mm/s doing 60 passes.

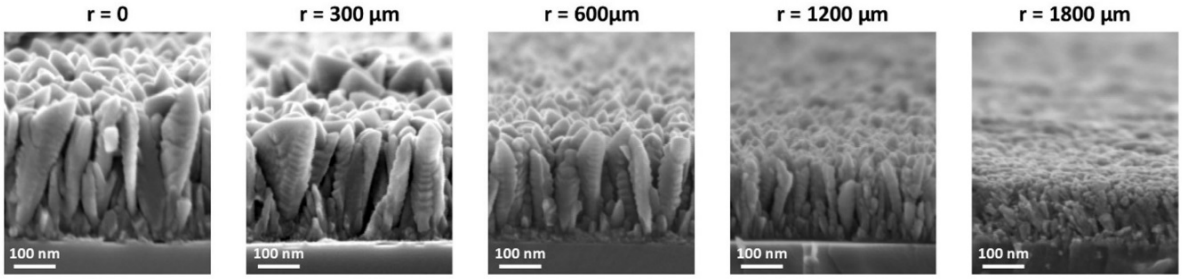

Fig. 12. Structure evolution from the center of the optimized film (r = 0 µm) to its peripheral zone.

3.3. Deposition of a square centimeter titania thin film

The structure composed of aligned titania monocrystals deposited on a coating line should be deposited on a square centimeter surface to make it useable for any application. The substrate was moved along both the *x* and the *y*-axis to achieve a homogeneous film. A first coating line was deposited with the previously optimized parameters (TTIP flow rate of 0.2 slpm), doing 8 passes along the *x*-axis, the substrate holder was then moved on 1 mm along the *y*-axis to deposit a second coating line along the *x*-axis, these steps were repeated until 10 coating lines were deposited (Fig. 13). It was verified that the coating thickness was homogeneous all over the coating despite the interference fringes appearing on its surface.

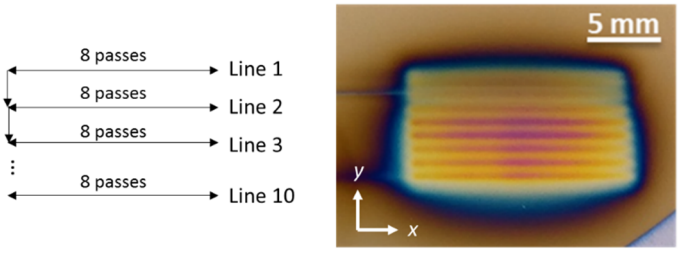

Fig. 13. Scheme and photo of a homogeneous TiO_2 coating doing 10 lines of 8 passes at 1 mm/s and 0.2 slpm of TTIP.

The thin film microstructure was observed by FESEM (Fig. 14). The rice-like surface structure is very similar to the surface of the coating line presented on the Fig. 7. The cross-section image shows the same aligned facetted columns as in the previous part. It could be assumed that each column is a titania monocrystal.

The elaboration of a square centimeter coating doing 8 passes on 10 consecutive lines permitted to achieve a 200 nm thick film, while 60 passes are necessary to achieve a simple coating line of 300 nm. Considering a simple coating line, a thickness of 40 nm is obtained with 8 passes, and its width is approximately 3 mm. Thus, during the square centimeter film elaboration, each deposited coating line receives the contributions of between 2 and 4 adjacent coating lines. In addition, other contributing factors have to be considered like the reactive species recirculation in the peripheral zone of the plasma jet and the thermal warm-up of the substrate.

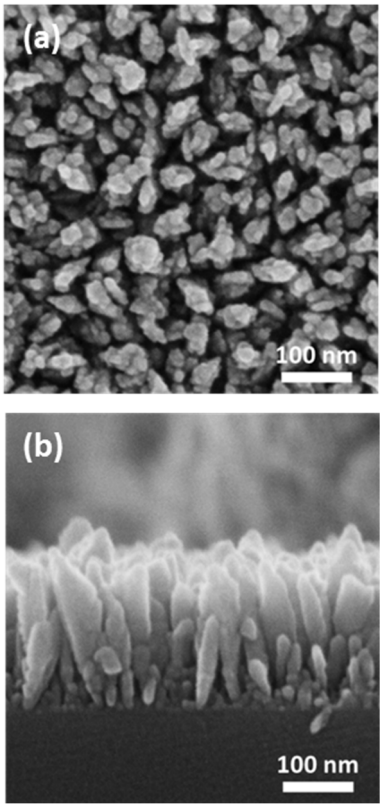

Fig. 14. FESEM images of the ~~surface~~ optimized titania film, (a) top view and (b) cross-section.

The polycrystalline nature of the coating was investigated by XRD analysis. The Fig. 15 pattern shows the same anatase (101) preferred orientation as before, and the presence of rutile phase is detected under the (110) plan. The phase proportions are calculated with the equations (1) and (2). It appeared that the film is composed of 90 % of anatase phase and 10 % of rutile phase. Contrary to the coating lines elaborated at 0.2 slpm, the film is mostly crystallized under the anatase phase. In this configuration, each substrate point may spend less time under the plasma and thus could not gather a sufficient amount of energy for the transition from anatase to rutile phase.

The surface reaction growth mechanism is dominant thanks to the optimized process parameters chosen before. In these conditions, the fluid dynamic changes induced by the substrate movement are no longer a challenge to deposit a large titania film composed of aligned monocrystals. The

homogeneous nucleation in the plasma phase is also sufficiently limited and the nanoparticles agglomeration on the peripheral zone of the film is avoided.

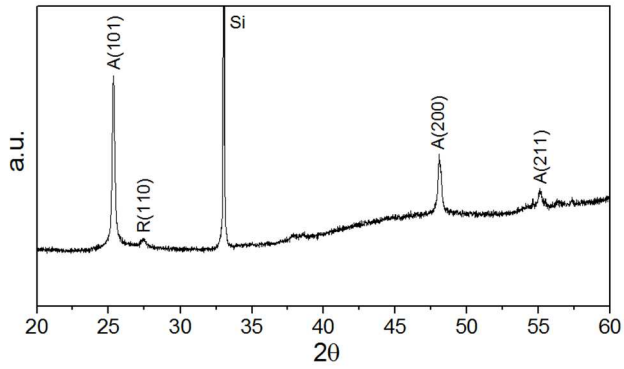

Fig. 15. XRD pattern of the square centimeter titania film elaborated in the optimized conditions.

4. Conclusion

The influence of the substrate movement along a coating line for titania deposition was studied and compared to static deposition. The optimization of the process parameters allowed to control the columns growth mechanisms. A slow moving speed of 1 mm/s was chosen to avoid disorder in the columns structure. Then the precursor flow rate was decreased to 0.2 slpm to promote the film growth by surface reaction. Indeed, decreasing the precursor flow rate allowed to limit the homogeneous nucleation in the plasma phase to switch from growth by nanoparticles agglomeration to growth by surface reaction. A columnar coating where each column is a titania crystal was obtained similarly to the static mode microstructure.

The main challenge was to deposit such a microstructure on a square centimeter surface to make it suitable to use in applications like photocatalysis or photovoltaics. Thus the previous optimized process parameters (1 mm/s, 0.2 slpm) were implemented on an x-y movement. A homogeneous columnar film was achieved, it is mostly crystallized under the anatase phase with an anatase (101) preferred orientation.

The next step of this work should be dedicated to the understanding of the links between the plasma chemistry and the thin film growth to investigate the step by step construction of the titania coating elaborated by the TIA. Deposited on an appropriate substrate, these well-crystallized films composed of aligned monocrystals seem ideal to be integrated into dye-sensitized or perovskite solar cells, since depositing a large surface is no longer an issue. The structural characteristics could enhance the electron transfer through the cell and improve its efficiency.

Acknowledgments

The authors would like to thank P. Carles from IRCER for the TEM analyses. They also gratefully acknowledge financial support granted by the Region Limousin and the laboratory of excellence ∑-Lim.

References

[1] J.C. Yu, J. Yu, W. Ho, J. Zhao, Light-induced super-hydrophilicity and photocatalytic activity of mesoporous TiO_2 thin films, J. Photochem. Photobiol. Chem. 148 (2002) 331–339. doi:10.1016/S1010-6030(02)00060-6.
[2] S. Collette, J. Hubert, A. Batan, K. Baert, M. Raes, I. Vandendael, A. Daniel, C. Archambeau, H. Terryn, F. Reniers, Photocatalytic TiO_2 thin films synthesized by the post-discharge of an RF atmospheric plasma torch, Surf. Coat. Technol. 289 (2016) 172–178. doi:10.1016/j.surfcoat.2016.01.049.
[3] M. Pelaez, N.T. Nolan, S.C. Pillai, M.K. Seery, P. Falaras, A.G. Kontos, P.S.M. Dunlop, J.W.J. Hamilton, J.A. Byrne, K. O'Shea, M.H. Entezari, D.D. Dionysiou, A review on the visible light active titanium dioxide photocatalysts for environmental applications, Appl. Catal. B Environ. 125 (2012) 331–349. doi:10.1016/j.apcatb.2012.05.036.
[4] X. Chen, S.S. Mao, Titanium dioxide nanomaterials: synthesis, properties, modifications, and applications, Chem Rev. 107 (2007) 2891–2959. doi:10.1021/cr0500535.
[5] A. Kumar, A.R. Madaria, C. Zhou, Growth of Aligned Single-Crystalline Rutile TiO_2 Nanowires on Arbitrary Substrates and Their Application in Dye-Sensitized Solar Cells, J. Phys. Chem. C. 114 (2010) 7787–7792. doi:10.1021/jp100491h.
[6] B. Liu, E.S. Aydil, Growth of Oriented Single-Crystalline Rutile TiO_2 Nanorods on Transparent Conducting Substrates for Dye-Sensitized Solar Cells, J. Am. Chem. Soc. 131 (2009) 3985–3990. doi:10.1021/ja8078972.
[7] X. Tong, F. Lin, J. Wu, Z.M. Wang, High Performance Perovskite Solar Cells, Adv. Sci. 3 (2016) 1500201. doi:10.1002/advs.201500201.
[8] M. Salado, M. Oliva-Ramirez, S. Kazim, A.R. González-Elipe, S. Ahmad, 1-dimensional TiO_2 nano-forests as photoanodes for efficient and stable perovskite solar cells fabrication, Nano Energy. 35 (2017) 215–222. doi:10.1016/j.nanoen.2017.03.034.
[9] W.A.A. Syed, N. Rafiq, A. Ali, R. Din, W.H. Shah, Multilayer AR coatings of TiO_2 /MgF_2 for application in optoelectronic devices, Opt. - Int. J. Light Electron Opt. 136 (2017) 564–572. doi:10.1016/j.ijleo.2017.02.085.
[10] M. Mazur, D. Wojcieszak, D. Kaczmarek, J. Domaradzki, S. Song, D. Gibson, F. Placido, P. Mazur, M. Kalisz, A. Poniedzialek, Functional photocatalytically active and scratch resistant antireflective coating based on TiO_2 and SiO_2, Appl. Surf. Sci. 380 (2016) 165–171. doi:10.1016/j.apsusc.2016.01.226.
[11] A. Sobczyk-Guzenda, M. Gazicki-Lipman, H. Szymanowski, J. Kowalski, P. Wojciechowski, T. Halamus, A. Tracz, Characterization of thin TiO_2 films prepared by plasma enhanced chemical vapour deposition for optical and photocatalytic applications, Thin Solid Films. 517 (2009) 5409–5414. doi:10.1016/j.tsf.2009.01.010.
[12] Y. Lee, J. Chae, M. Kang, Comparison of the photovoltaic efficiency on DSSC for nanometer sized TiO_2 using a conventional sol–gel and solvothermal methods, J. Ind. Eng. Chem. 16 (2010) 609–614. doi:10.1016/j.jiec.2010.03.008.
[13] A.M. Gaur, R. Joshi, M. Kumar, Deposition of Doped TiO_2 Thin Film by Sol Gel Technique and its Characterization: A Review, Lect. Notes Eng. Comput. Sci. 2191 (2011). http://www.iaeng.org/publication/WCE2011/WCE2011_pp1500-1503.pdf.
[14] R. Alvarez, P. Romero-Gomez, J. Gil-Rostra, J. Cotrino, F. Yubero, A.R. Gonzalez-Elipe, A. Palmero, Growth of SiO_2 and TiO_2 thin films deposited by reactive magnetron sputtering and PECVD by the incorporation of non-directional deposition fluxes, Phys. Status Solidi A. 210 (2013) 796–801. doi:10.1002/pssa.201228656.
[15] Y.-M. Sung, Deposition of TiO_2 Blocking Layers of Photovoltaic Cell Using RF Magnetron Sputtering Technology, Energy Procedia. 34 (2013) 582–588. doi:10.1016/j.egypro.2013.06.788.
[16] S. Mathur, P. Kuhn, CVD of titanium oxide coatings: Comparative evaluation of thermal and plasma assisted processes, Surf. Coat. Technol. 201 (2006) 807–814. doi:10.1016/j.surfcoat.2005.12.039.
[17] R. Tu, T. Goto, High temperature stability of anatase films prepared by MOCVD, Mater. Trans. 49 (2008) 2040–2046. doi:10.2320/matertrans.MRA2008114.

[18] K.L. Choy, Chemical vapour deposition of coatings, Prog. Mater. Sci. 48 (2003) 57–170. doi:10.1016/S0079-6425(01)00009-3.
[19] M. Wu, Y. Xu, L. Dai, T. Wang, X. Li, D. Wang, Y. Guo, K. Ding, X. Huang, J. Shi, J. Zhang, The Gas Nucleation Process Study of Anatase TiO_2 in Atmospheric Non-Thermal Plasma Enhanced Chemical Vapor Deposition, Plasma Sci. Technol. 16 (2014) 32–36. doi:10.1088/1009-0630/16/1/07.
[20] Y. Gazal, C. Dublanche-Tixier, C. Chazelas, M. Colas, P. Carles, P. Tristant, Multi-structural TiO_2 film synthesised by an atmospheric pressure plasma-enhanced chemical vapour deposition microwave torch, Thin Solid Films. 600 (2016) 43–52. doi:10.1016/j.tsf.2016.01.011.
[21] R. Maurau, N.D. Boscher, S. Olivier, S. Bulou, T. Belmonte, J. Dutroncy, T. Sindzingre, P. Choquet, Atmospheric pressure, low temperature deposition of photocatalytic TiO_x thin films with a blown arc discharge, Surf. Coat. Technol. 232 (2013) 159–165. doi:10.1016/j.surfcoat.2013.05.001.
[22] N.D. Boscher, S. Olivier, R. Maurau, S. Bulou, T. Sindzingre, T. Belmonte, P. Choquet, Photocatalytic anatase titanium dioxide thin films deposition by an atmospheric pressure blown arc discharge, Appl. Surf. Sci. 311 (2014) 721–728. doi:10.1016/j.apsusc.2014.05.145.
[23] H. Fakhouri, D.B. Salem, O. Carton, J. Pulpytel, F. Arefi-Khonsari, Highly efficient photocatalytic TiO_2 coatings deposited by open air atmospheric pressure plasma jet with aerosolized TTIP precursor, J. Phys. Appl. Phys. 47 (2014) 265301. doi:10.1088/0022-3727/47/26/265301.
[24] S.S. Asad, J.P. Lavoute, C. Dublanche-Tixier, C. Jaoul, C. Chazelas, P. Tristant, C. Boisse-Laporte, Deposition of Thin SiO_x Films by Direct Precursor Injection in Atmospheric Pressure Microwave Torch (TIA), Plasma Process. Polym. 6 (2009) S508–S513. doi:10.1002/ppap.200931104.
[25] Y. Gazal, C. Chazelas, C. Dublanche-Tixier, P. Tristant, Contribution of optical emission spectroscopy measurements to the understanding of TiO_2 growth by chemical vapor deposition using an atmospheric-pressure plasma torch, J. Appl. Phys. 121 (2017) 123301. doi:10.1063/1.4979024.
[26] X. Landreau, C. Dublanche-Tixier, C. Jaoul, C. Le Niniven, N. Lory, P. Tristant, Effects of the substrate temperature on the deposition of thin SiO_x films by atmospheric pressure microwave plasma torch (TIA), Surf. Coat. Technol. 205 (2011) S335–S341. doi:10.1016/j.surfcoat.2011.03.123.
[27] J.L. Hodgkinson, H.M. Yates, A. Walter, D. Sacchetto, S.-J. Moon, S. Nicolay, Roll to roll atmospheric pressure plasma enhanced CVD of titania as a step towards the realisation of large area perovskite solar cell technology, J. Mater. Chem. C. 6 (2018) 1988–1995. doi:10.1039/C8TC00110C.
[28] A. Borras, J.R. Sanchez-Valencia, R. Widmer, V.J. Rico, A. Justo, A.R. Gonzalez-Elipe, Growth of Crystalline TiO_2 by Plasma Enhanced Chemical Vapor Deposition, Cryst. Growth Des. 9 (2009) 2868–2876. doi:10.1021/cg9001779.
[29] L. Romero, R. Binions, Effect of AC electric fields on the aerosol assisted chemical vapour deposition growth of titanium dioxide thin films, Surf. Coat. Technol. 230 (2013) 196–201. doi:10.1016/j.surfcoat.2013.05.026.
[30] J.L. Hodgkinson, D.W. Sheel, Advances in atmospheric pressure PECVD: The influence of plasma parameters on film morphology, Surf. Coat. Technol. 230 (2013) 73–76. doi:10.1016/j.surfcoat.2013.06.079.
[31] C. Jiménez, D. De Barros, A. Darraz, J.-L. Deschanvres, L. Rapenne, P. Chaudouët, J.E. Méndez, F. Weiss, M. Thomachot, T. Sindzingre, G. Berthomé, F.J. Ferrer, Deposition of TiO_2 thin films by atmospheric plasma post-discharge assisted injection MOCVD, Surf. Coat. Technol. 201 (2007) 8971–8975. doi:10.1016/j.surfcoat.2007.04.025.
[32] R.A. Spurr, H. Myers, Quantitative analysis of anatase-rutile mixtures with an X-ray diffractometer, Anal. Chem. 29 (1957) 760–762. doi:10.1021/ac60125a006.